

Mechanical, Rheological, Morphological and Frictional Properties of Cast Iron Coated by HVOF Method

Mehmet ÇAKMAKKAYA¹ Ahmet ÇETKİN²Department of Automotive Engineering, Faculty of Technology, Afyon Kocatepe University, Turkey¹Department of Mechanical Engineering, Faculty of Technology, Afyon Kocatepe University, Turkey²

ABSTRACT: In this study, mechanical, rheological and morphological properties of cast iron, containing 3.8% carbon, coated by High Speed Oxygen Fuel (HVOF) method were investigated. 45 μ m Cr₃C₂- 25% NiCr and WC-% 12Co sintered powders were used for coating the surfaces. The microstructure of the coated surfaces was characterized by scanning electron microscopy at each step. By means of finite element method, the temperature distributions on the surfaces were determined and the changes in the rheological and morphological properties were also tested. It has been determined that the mechanical, rheological and frictional properties of the coated samples are better than those of uncoated brake pads.

KEYWORDS: Finite element, HVOF, thermal and mechanic properties, rheology, morphology

I. INTRODUCTION

WC-12Co coatings made by plasma spraying method are widely used in various fields depending on their fields such as chemical inertness, high hardness, abrasion resistance, high elasticity and low friction (F. Ghadami, 2013). Coatings formed by plasma spraying have many disadvantages in actual applications, such as the porous structure formed on the coating surface and the formation of the coating due to poor adhesion to the surface (Y. Wang, 2009). The formation of porous structures greatly reduces the hardness and wear resistance of the coating. As a result of the poor adhesion of the coating surface, the coating material tends to peel off the coating layers from the underlying layer if the coating material is subjected to a heavy load or high bending stress (F. Ghadami, 2010). The laser melting process can significantly increase plasma properties, removing layered structures of sprayed coatings by lifting the pores and cracks in the middle, thereby creating a metallurgical combination between the coatings and the substrate (C. Cui, 2012). In remelting processes, the laser creates a molten pool due to intense heating in the laser-induced local area. As the laser beam moves along the coating surface, the molten pool will also move along the laser beam. Obviously, the temperature profile in the laser-generated molten pool has significant effects on convection heat and mass transfer. This affects the solidification process, the homogenization of the composition and the microstructure of the coatings. However, due to the rapid heating and cooling rate, it is extremely difficult to experimentally measure the temperature change and the actual size of the molten pool. For this reason, theoretical simulations of the laser remelting process have become imperative. The three dimensional (3D) finite element methods are widely used to simulate the time dependence of the temperature field over the laser-induced molten pool. For example, the temperature distribution, melt pool dimensions and stress area have been determined during the melting of a wide variety of coatings and surfaces by laser (H. F. Guo, 2016). These are Al-weighted 1.5% Fe alloys (F. Bertelli, 2011), 42CrMo4 steel (CW Li, 2010), HVOF WC mixture coating (Akhtar, 2012), Q235 mild steel (P. Yi, 2011), 42CrMo steel -Z Zhan, 2009), 33% Cu eutectic alloy by weight (O. Satbhai, 2012). In these studies, 3D FEM method was used and this model was verified by experimental work, a WC-12Co coating was prepared on the brake discs made of gray cast iron with HVOF, and the morphologies, chemical element distributions and coating phases of the surface coating formed were determined by scanning electron microscopy (SEM), energy dispersive spectrometry (EDS) and X-ray diffraction analyzed.

International Journal of Innovative Research in Science, Engineering and Technology

(An ISO 3297: 2007 Certified Organization)

Vol. 6, Special Issue 10, May 2017

II. EXPERIMENTAL PROCEDURE

In this study, the wear behaviors of automobile brake discs and the dual performance of brake disc and brake pads in braking process were investigated. For this purpose, cast iron-made discs with spectral analysis in Table 1 were used. The cermet coatings used for these discs provide a wide range of suitable solutions for the wear resistance. Such coated materials are made more performance by being protected from environmental and physical effects in the working area. Coating processes with WC-% 12Co and Cr3C2-% 25NiCr materials are commonly developed coatings for gas turbines, steam turbines and aero-engineers. Such coating materials provide better performance by protecting the area of operation from environmental and physical adverse effects. The roughness values of the coated discs increase after the test, ensuring better adhesion with the brake pads during braking operation. On the coated disc, the surface roughness decreased. Besides, it has been found that the coated surfaces form a thermal barrier during braking and accordingly, the braking distance increases. The temperature distributions determined by the Finite Elements Method also confirm the extent of the braking distance. The thermal variables that occur at the disk surface are given in Figures 6-7.

Table 1. Spectral analysis values of brake disc used in experimental study

Elementler	C	Si	Mn	P	S	Cr	Mo	Ni	Cu	Ti	Fe
% oranları	3.83	2.227	0.791	0.031	0.139	0.150	0.022	0.012	0.026	0.019	92.692

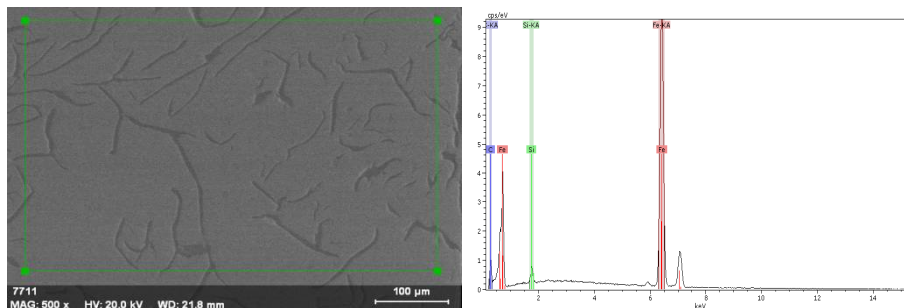


Figure 1. SEM image of original disc

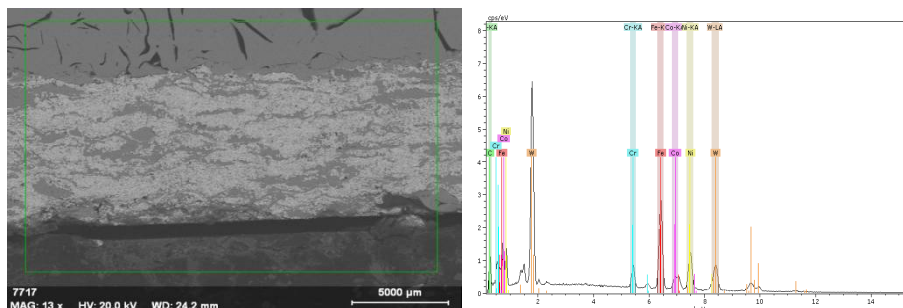


Figure 2. SEM images of WC-%12Co coated disc

International Journal of Innovative Research in Science, Engineering and Technology

(An ISO 3297: 2007 Certified Organization)

Vol. 6, Special Issue 10, May 2017

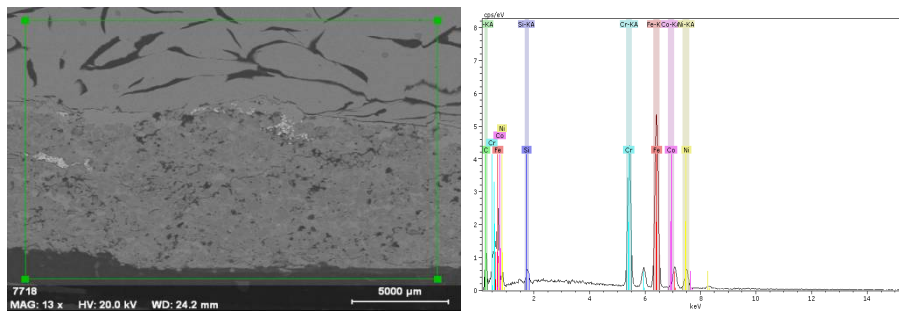


Figure 3. SEM images of Cr₃C₂-%25NiCr coated disc

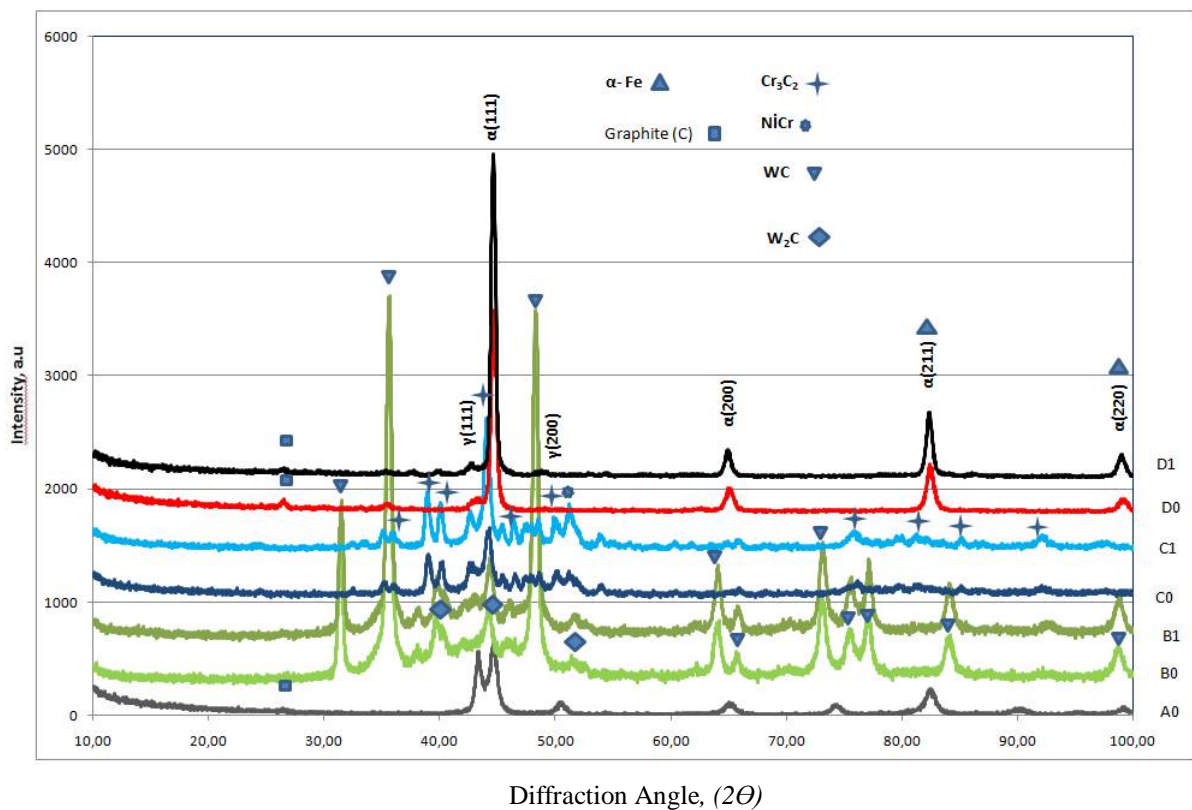
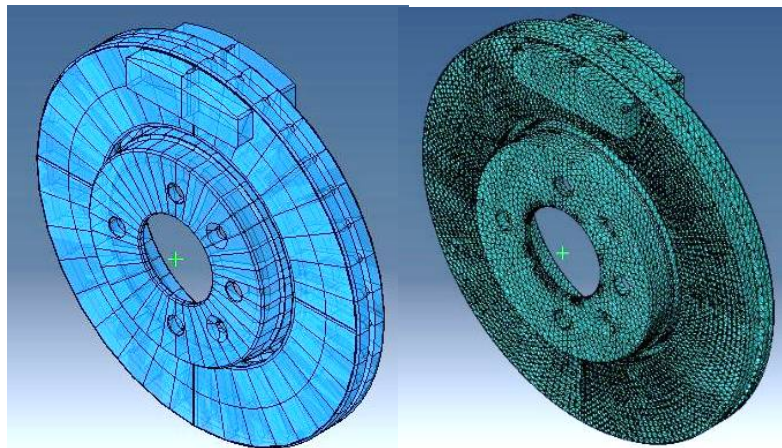


Figure 4. XRD analysis of discs

International Journal of Innovative Research in Science, Engineering and Technology

(An ISO 3297: 2007 Certified Organization)

Vol. 6, Special Issue 10, May 2017



(a) (b)
Figure 5.FEM geometries of disc and pads

Pads and disk geometry modelled in the problem are given in figure 5a and the mesh structures for the application of the finite element technique of these geometries are also given in figure 5b. The ABAQUS that we use for finite element analysis program is based on the static, dynamic, heat transfer, acoustics problems and their dynamic and pseudostatic problems, nonlinear heat flow, structural flow, advanced dynamics of computational fluids other than the modules required by some customers is a finite element pre & post software developed for solving problems. A very small element size structures are included about 165000 nodes for the mesh was determined. For the Coupled Temperature-Displacement solution technique from the standard element library, the C3D4T element in the linear geometric structure is used. This element type of the ABAQUS program has a total of four solution nodes for each element. The mechanical and thermal properties of the materials used in the analysis are detailed in Table 2. The cast iron given in Table 1 for spectral analysis is the material used in the production of the brake discs. The thermo-mechanical properties used in the analysis for disc coating materials WC-%12Co and Cr3C2-%25NiCr, brake disc and brake pads are given in Table 2 in detail.

Table 2. Mechanical and Thermal Properties of Materials Used in Analysis

Mechanical and Thermal Properties	Materials			
	Cast Iron	Cr ₃ C ₂ -%25NiCr	WC-%12Co	Pad
Modulus of Elasticity (N/m ²)	2.09x10 ¹¹	34.5 x10 ¹¹	6.5x10 ¹¹	2.20x10 ⁸
Poisson Ratio (m/m)	0.30	0.20	0.30	0.25
Density (kg/m ³)	7920	6680	13900	1550
Thermal Expansion Coefficient (1/°C)	1.1x10 ⁻⁵	1.04x10 ⁻⁵	5.0x10 ⁻⁶	1.0x10 ⁻⁵
Specific Heat (J/Kg ⁰ C)	452	182	126	1200
Thermal Conductivity Coefficient (J/s/m ⁰ C)	48	19	34.4	0.9
Thermal Conductivity (in Contact)	5x10 ¹²	5x10 ¹²	5x10 ¹²	5x10 ¹²

Depending on the properties of the disc, pads and coating materials used in the analysis, the energy generated by the contact is completely converted into heat and the heat dissipated to the brake disk and the brake pads in different ratios. For an incomplete contact state, this distribution ratio is;

$$\epsilon = \frac{\epsilon_d \cdot S_d}{\epsilon_d \cdot S_d + \epsilon_b \cdot S_b} \quad \text{Equation 1.}$$

In this equation, S_d and S_b are the contact surface areas for the brake disc and the brake pads, respectively. Thermal dispersion ratio is;

International Journal of Innovative Research in Science, Engineering and Technology

(An ISO 3297: 2007 Certified Organization)

Vol. 6, Special Issue 10, May 2017

$$\varepsilon = \sqrt{k \cdot \rho \cdot c}$$

Equation 2.

In this equation, ρ , c , k denote the density, thermal conductivity and specific heat, respectively. The values obtained for the heat distribution ratios between the brake disk, the coating and the pads are given in Table 3. Same table also shows the direction of the thermal flow towards the contact material and the percent value of the heat dissipated here in the first column (F. Talafi, 2009).

Table 3. Thermal Distribution Rates on Surfaces

Contacting materials	Distribution Rate (%)	
Disc-WC-% 12Co	62.81	37.19
Disc-Cr ₃ C ₂ -% 25NiCr	73.17	26.83
Pad -WC-% 12Co	14.29	85.71
Pad-Cr ₃ C ₂ -% 25NiCr	21.21	78.79
Pad-Disc	8.98	91.02

The temperature generated by contact is distributed by convection, thermal radiation and thermal conduction from the contact area. Since the brake disc has reached a certain speed and it is in contact with air, the heat generated in the brake disc is transferred to the air and the pads by convection. The coefficient that defines the temperature at which the brake disc is released into the air at the specified test speed;

$$h_{ns} = 10.45 + 10 \cdot \sqrt{V} - V$$

Equation 3.

This value was taken as 23.298 for the friction surfaces as shown in Table 4 for the test speed (250 rpm). The convection coefficient in pads and other areas of the brake disc is given in the literature as 0.068 in terms of stagnant air (D. Majcherczag, 2005).

Table 4. Convection coefficients on contact surfaces (W/m²h⁰C)

Surfaces	Convective heat transfer coefficient
Friction Surfaces	23.298
Free Surfaces	0.068

The coefficient of friction of the pads, disc and coating materials measured in relation to each other naturally varies at different temperatures, different speeds and different contact pressures. The results obtained from the experiments are given in Table 5.

Table 5. Friction coefficient of the contacted materials

Materials	Friction coefficient	Discspeed (m/sn)	Contact Pressure (N/m ²)	Temperature (°C)
Disc-Pad	0.60	13.89	1.4x10 ⁶	100
	0.45	27.78	1.6x10 ⁶	120
	0.41	44.44	1.8x10 ⁶	300
Pad-Coating (WC-% 12Co)	0.50	13.89	1.4x10 ⁶	100
	0.45	27.78	1.6x10 ⁶	120
	0.53	44.44	1.8x10 ⁶	250
Pad-Coating (Cr ₃ C ₂ -% 25NiCr)	0.56	13.89	1.4x10 ⁶	117
	0.49	27.78	1.6x10 ⁶	240
	0.46	44.44	1.8x10 ⁶	327

International Journal of Innovative Research in Science, Engineering and Technology

(An ISO 3297: 2007 Certified Organization)

Vol. 6, Special Issue 10, May 2017

ABAQUS software gives the resulting temperatures for at each nodes (NT) and elements (TEMP). In this study, transient thermal analysis results were evaluated on an element basis. The initial temperature values of all the objects used in the analysis are given as 20°C. Again the same value was taken for the sink temperature required for convection. Since the dimensions of the simple geometry pads used in the experiments differ from the standard pad type geometry used in the analysis, the pressure value of the pad was recalculated according to the new geometry and used for analysis at 5.798×10^6 Pa.

The analysis was studied in two steps; the solution was carried out until the pressure reached the maximum value at the first step of the analysis, while the other step of the analysis was fixed at the last position, while the disc was given an angular velocity of 250 rpm. The Coupled Temperature-Displacement analysis structure was used for both analysis steps and the results of the transient thermal analysis were calculated using the Full Newton solution technique. In the analysis, the temperature values are given for the original and uncoated state of the disk surface, as well as the coated states of WC-%12Co and Cr₃C₂-%25NiCr coating materials for three different numbers of turns. Table 6 shows how the temperature distributes on the inside of the brake disc when the temperature distribution on the outer surface of the disc is given from an isometric point of view. Obtained analysis results clearly show that the coated and uncoated disc have very different thermal distribution structures on the surface of the disc or inside the disc. The brake disc structure coated with both coating materials shows a similarity with very small differences. In the case of discs with no coating material in the first half turn, the maximum temperature value is 56 °C at the surface. At the end of the two turns, these values show up to about 82 °C on uncoated discs and up to about 169 °C on coated discs.

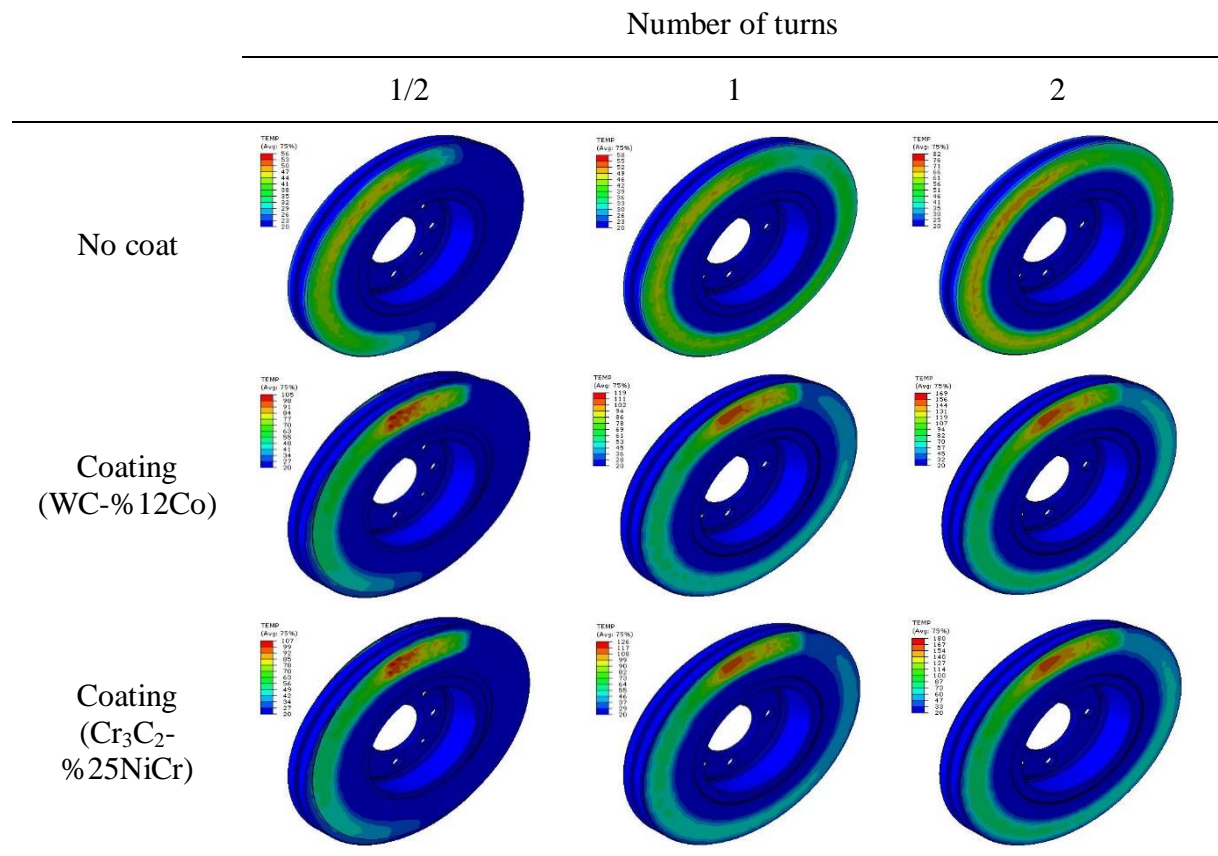


Figure 6 Temperature distributions on outer surface of the brake disc

International Journal of Innovative Research in Science, Engineering and Technology

(An ISO 3297: 2007 Certified Organization)

Vol. 6, Special Issue 10, May 2017

Number of turns

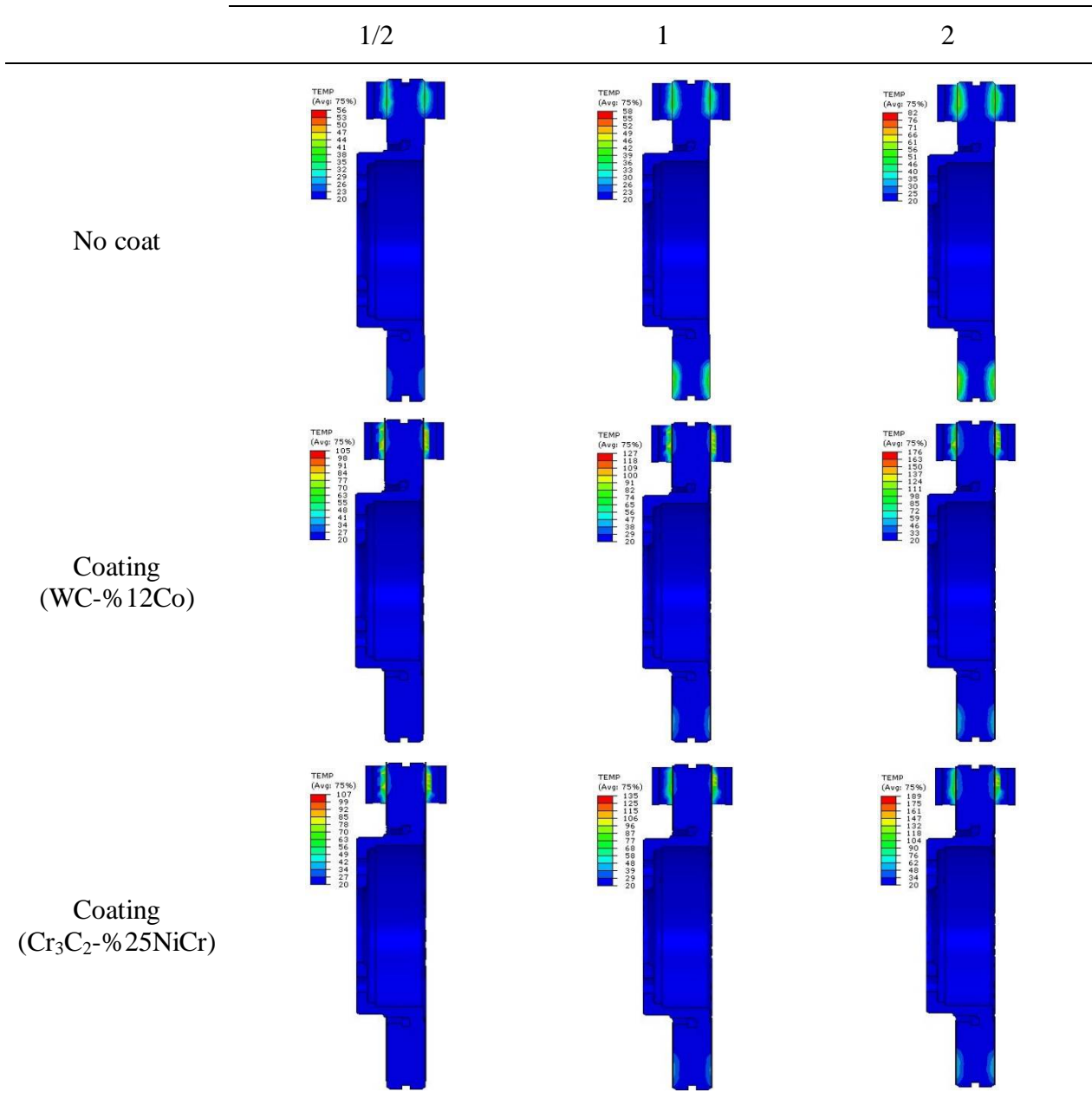


Figure 7. Temperature distributions within the brake disk

International Journal of Innovative Research in Science, Engineering and Technology

(An ISO 3297: 2007 Certified Organization)

Vol. 6, Special Issue 10, May 2017

III. CONCLUSION

- i. In the study, the discs coated with Cr₃C₂-% 25NiCr and WC-% 12Co cermet powders were observed to have high wear resistance as expected for surface wear during braking tests. However, the reduction in the thickness of the brake pad material used as an abrasive is less in the case of coated discs.
- ii. When coating with Cr₃C₂-%25 NiCr and WC-%12Co with HVOF, the coating layer formed on the brake disc surface reduces the friction coefficient. As a result, there is an increase in braking distance. The resulting increase in braking distance is due to the fact that the resin that forms the break pad material has a shorter duration of softening due to the thermal barrier effect on the coated surface.
- iii. If the resin used in the production of break pad is resistant to high temperatures or the use of dual pads for coating cermet powders, the braking distance will also be achieved at desired break levels.
- iv. The decrease in thickness at the start was 4.21 mm for uncoated discs, while the decrease in disc thickness covered by cermet powder was 2.59 mm. If suitable brake pad material is chosen, such coated discs can be used for longer life.

REFERENCES

- [1] Akhtar, B. Y. (2012). Laser re-melting of HVOF coating with WC blend: thermal stress analysis. *J. Mater. Process. Technol.*, 2569-2577.
- [2] C. W. Li, Y. W. (2010). Three- dimensional finite element analysis of temperatures and stresses in wide-band laser surface melting processing. *Mater. Des.*, 3366-3373.
- [3] C.Cui, F. X. (2012). Laser surface remelting of Fe based alloy coating deposited by HVOF. *Surf. Coat. Technol.*, 2388-2395.
- [4] D. Majcherczag, P. D.-A. (2005). Third Body Influence on Thermal Friction Contact Problems: Application to Braking. *Journal Tribol* 127, 89-95.
- [5] F. Bertelli, e. s. (2011). Laser remelting of Al-1.5 wt % Fe alloy surfaces: numerical and experimental analyses. *Opt. Laser Eng.*, 490-497.
- [6] F. Ghadami, S. a.-P. (2013). Structural and oxidation behavior of atmospheric heat treated plasma sprayed Wc-Co coatings. *Vacuum*, 64-68.
- [7] F. Talafi, 2. (2009). Analysis of heat conduction in a disk breke system. *Heat Mass Transfer*, V.45, 1047- 1059.
- [8] F.Ghadami, M. H. (2010). Comparative tribological study of air plasma sprayed WC-12%Co coating versus conventional hard chromium electrodeposit. *Tribol. Int.*, 882-886.
- [9] H. F. Guo, Z. J. (2016). laser surface remelting of WC-12 Co coating: finite element simulations and experimental analyses. *materials Science and Technology*, 813-822.
- [10] H.-Z. Zhan, Y. C.-W.-M. (2009). Computational and experimental study of a melt-hardened zone on a roller modified by wide-band laser treatment. *Opt. Laser Technol.*, 251-257.
- [11] O. Satbhai, S. R. (2012). Numerical simulation of laser surface remelting on unstructured grids. *Trans. Indian Inst. Met.*, 833-840.
- [12] P. Yi, Y. C. (2011). Effects analysis of ambient conditions on process of laser surface melting. *Opt.Laser Technol.*, 1411-1419.
- [13] Y. Wang, C. G. (2009). Laser surface remelting of plasma sprayed nanostructured Al₂O₃-13wt %TiO₂ coating on titanium alloy. *Appl. Surf. Sci.*, 8603-8610.